Proceedings of CHT-17
ICHMT International Symposium on Advances in Computational Heat Transfer

May 28-June 1, 2017, Napoli, Italy

CHT-17-xxx

INVESTIGATION OF THE EFFECT OF BROWNIAN MOTION ON THE FLOW CHARACTERISTIC IN NATURAL CONVECTION USING DIFFERENT NANOFLUIDS

Saleh Etaig[**,§], Reaz Hasan[*], Noel Perera[*] and Ahmed Ramadan[*]
[*]Mechanical and Construction Engineering Department, Northumbria University. Newcastle, UK
[**]Mechanical Engineering Department, University of Benghazi, Benghazi. Libya
[§]Correspondence author. Fax: +441912326002 Email: Salehorafi@yahoo.com

ABSTRACT This paper reports the effect of the Brownian motion on the fluid flow and heat transfer performance using various nanofluids in a natural convection in square enclosure. The energy equation and Navier-Stokes equation are solved numerically using finite volume approach. The effect of the Brownian motion was employed based on thermal conductivity model with Brownian motion effect. The effect of volume concentration on the enhancement of heat transfer has been studied incorporating the Brownian motion; the influence of effective thermal conductivity on the enhancement was also investigated for a range of volume fraction concentration. Various volume concentrations were tested in the present study; 2%, 3%, 4% and 6%. Different Raleigh numbers were investigated for different nanoparticles. The results revealed that the increase in the volume fraction deteriorates the heat transfer. The velocity gradients were also found to be affected by the volume fractions. The temperature profile for different Rayleigh number is presented. Three different nanofluids Cu-Water, TiO-water and AL2O3-water were studied.

Keywords:
Heat Transfer, CFD, Natural convection and Brownian motion

Introduction

The natural convection heat transfer arises within an enclosure due to the temperature difference and buoyancy force, one of the limitations of enhancing the heat transfer of the natural convection is the intrinsically low thermal conductivity of the conventional fluids.
The Nanofluids are suspensions with less than 100 nanometer diameter. The pioneering work in introducing this new class of these fluids was first done by Choi (Choi and Eastman, 1995) and it was when he coined the term nanofluid. Nanofluids are dilute suspensions of. Nanofluids have been found to retain enhanced thermophysical properties of the fluid, these properties are: thermal conductivity, viscosity, density and heat capacity. Furthermore, the convective heat transfer coefficient was found increased in comparison to those of base fluids like oil or water. It has demonstrated feasible applicability in many fields such as electronic applications, industrial systems cooling, heating building, nuclear systems cooling and many other applications.
The investigation of the enhancement of heat transfer due to the use of nanofluids has recently attracted the attention of many researchers (Xuan and Li, 2000)-(Khanafer et al., 2003).. Putra et al (Putra et al., 2003) observed the natural convective characteristics of water based Al2O3 nanofluids, they reported that adding nanoparticles to base fluid systematically worsen the natural convective

heat transfer with the increase in nanoparticle concentration. However, they did not give an acceptable reason for decrease of the natural convective heat transfer in a cavity with the increment of the volume fraction of nanoparticles. According to many literature investigations the thermal conductivity is found to be the most affecting key role in the enhancement utilizing nanofluids, the effective thermal conductivity was modelled using theoretical and experimental models of nanofluids. Saleh et al. (Saleh et al., 2011) investigated the natural convection in trapezoidal filled with nanofluids. Nasrin et al. (Nasrin et al., 2012) investigated the heat transfer performance in a vertical closed enclosure and it is found that the nanoparticle volume fraction play a significant role on the temperature field. Ghasemi and Aminossadati (Ghasemi and Aminossadati, 2009) carried out a numerical study and investigated on natural convection heat transfer in an inclined enclosure filled with CuO–water nanofluids. Ho et al. (Ho et al., 2010) investigated experimentally the natural convection heat transfer of Al2O3-water based nanofluid. Ghasemi et al. (Ghasemi and Aminossadati, 2010) studied the effect of the effect of the Brownian motion in a triangular enclosure with natural convection.

Manca et al (Manca et al., 2001) conducted an experimental investigation on Air natural convection on a vertical isoflux plate with a downstream unheated extension and a facing parallel shroud. They reported an improvement in the thermal performance in most of configurations of the channel.

Sarris et al. (Sarris et al., 2004) presented a numerical investigation to give a better understanding of some aspects of natural convection in a glass melting tank heated locally from below. They tested the effects of location of heated strip by placing it at center and off center positions at the tank bottom wall. The highlighted that for small Rayleigh numbers, the heat transfer is dominated by conduction, while at higher Ra0 convection becomes dominant

Aminossadati and Ghasemi (Aminossadati and Ghasemi, 2009) studied numerically the natural convection in a square enclosure filled with CuO-water nanofluid with volume fractions up to 4%. They assumed the side and top walls as insulated. They divided the bottom wall into four sections. Based on the position of hot and cold parts, two cases were considered. They found that the increase in Rayleigh numbers promotes the natural convection flows and hence reduced the heat source temperature.

Oztop and Abu-Nada (Oztop and Abu-Nada, 2008) presented numerical simulations of natural convection in a partially heated rectangular cavity filled with nanofluids, they considered the effect of nanoparticle types in water base fluid (Cu Al2O3 and TiO2), volume concentration of nanoparticles and temperature fields. In their numerical study, heat source with finite length was placed on the left side with higher temperature than the right side. They reported that the level of heat transfer improves with increasing the Rayleigh number within the range 10^3–5×10^5 and the heater size.

Sun and Pop (Sun and Pop, 2011) studied the problem of natural convection heat transfer of a right angle triangular enclosure filled with a porous medium and filled by a nanofluid was numerically investigated by. For the enclosure, the heat source is located on the vertical wall, the inclined wall is cold with a fixed temperature and the vertical wall is adiabatic respectively. They tested the three same types of nanoparticles such as Cu, Al2O3 and TiO2 and the effect of nanoparticle volume fraction. They studied the effect of Rayleigh number for porous medium, heater size and enclosure aspect ratio as well. They reported that Nusselt number had a maximum value with both highest Ra number and largest heater size. Heat transfer is enhanced within the cavity with decreasing the enclosure aspect ratio and lowering the heat source. Furthermore, Cu based nanofluid performed as the better nanofluid for heat transfer.

The aim of this paper is to investigate the heat transfer enhancement in natural convection in a square enclosure with different nanoparticles types and incorporating the Brownian motion.

Problem Description

A schematic diagram of the physical domain is shown in Fig. 1. The model consists of a square enclosure with length and height equal to L. the upper and bottom walls are thermally insulated, the left wall is heated at temperature TH and right wall is maintained at lower temperature TC. the enclosure is filled with water based nanofluid, the nanoparticle investigated are: Al2O3, Cu and TiO2 with spherical diameter of 25 nm. The water and the nanoparticle are assumed in thermal equilibrium, Newtonian and incompressible, the flow is laminar, and the thermophysical properties are assumed temperature dependent and shown in the following section. The thermal properties of Al2O3, Cu and TiO2 particles are shown in Table I.

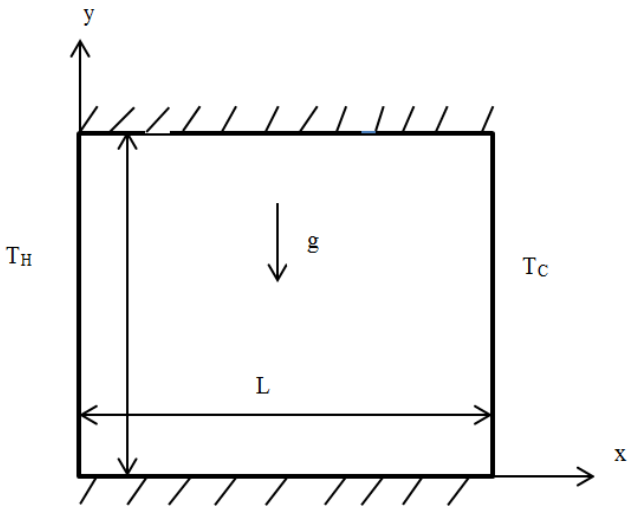

Figure 1 Problem Geometry

Governing Equations

The governing equations were solved in the present study are continuity, momentum equation and energy equation and can be written as

$$\frac{\partial \rho}{\partial t} + \boldsymbol{\nabla}.(\rho \boldsymbol{V}) = 0 \tag{1}$$

The momentum equation as expressed as:

$$\frac{\partial}{\partial t}(\rho \boldsymbol{V}) + \boldsymbol{\nabla}.\rho \boldsymbol{V}\boldsymbol{V} = \boldsymbol{\rho}\mathbf{f} + \boldsymbol{\nabla}.\mathrm{P}_{ij} \tag{2}$$

The energy equation

$$\frac{\partial E_t}{\partial t} + \boldsymbol{\nabla}.\mathrm{E_t}\mathbf{V} = \frac{\partial Q}{\partial t} - \boldsymbol{\nabla}.\mathbf{q} + \rho \mathbf{f}.\mathbf{V} + \boldsymbol{\nabla}.(P_{ij}.\mathbf{V}) \tag{3}$$

The thermophysical properties of the nanofluid are expressed as:
The density is calculated as

$$\rho_{nf} = (1-\phi)\rho_f + \emptyset\rho_s \quad (4)$$

The specific heat is written as:

$$C_{pnf} = \frac{(1-\emptyset)(\rho C_p)_f + \emptyset(\rho C_p)_s}{\rho_{eff}} \quad (5)$$

The thermal conductivity is modeled as:

$$K_{eff} = K_{static} + K_{Brownian} \quad (6)$$

The static thermal conductivity can be written as (Corcione et al., 2013)

$$\frac{K_{static}}{K_f} = 1 + 4.4Re^{0.4}Pr^{0.66}\left(\frac{T}{T_{fr}}\right)^{10}\left(\frac{K_s}{k_f}\right)^{0.03}\emptyset^{0.66} \quad (7)$$

The Brownian thermal conductivity is expressed as (Koo and Kleinstreuer, 2004)

$$K_{Brownian} = 5\times10^4\beta\emptyset\rho_f C_{pf}\sqrt{\frac{KT}{\rho_s d_s}}f(T,\emptyset) \quad (6)$$

K_b is the Boltzmann constant=1.3807x10^{-23}

$$\beta = 0.0011(100\emptyset)^{-0.7272} \quad (7)$$

Re number is calculated in equation (4.6) as:

$$Re = \frac{2\rho K_b T}{\pi\mu_f^2 d_p} \quad (8)$$

Where d_p s the particle diameter; Pr is the Prandtl number for base fluid and written as:

$$Pr = \frac{\mu C_p}{K} \tag{9}$$

The temperature function in equation (4.8) is given by:

$$f(T, \emptyset) = (-6.04\emptyset + 0.405)T + (1722.3\emptyset - 134.63) \tag{10}$$

The viscosity in this investigation is modelled as proposed by Etaig et al (Etaig et al., 2016) :

$$\mu_{static} = \mu_f(1 + 5\emptyset + 80\emptyset^2 + 160\emptyset^3) \tag{11}$$

The effective viscosity is calculated as:

$$\mu_{eff} = \mu_{static} + \mu_{Brownian} \tag{12}$$

Where d_f and d_s are the equivalent diameter of the base fluid and nanoparticle diameter respectively. The equivalent diameter of the base fluid is given by:

$$d_f = 0.1\left(\frac{6M}{N\pi\rho_{fo}}\right)^{\frac{1}{3}} \tag{13}$$

M is the molecular mass weight of the base fluid, N is the Avogadro number, ρ_{fo} is the mass density of the base fluid calculated at T=293 K. The Brownian viscosity is calculated as

$$\mu_{Brownian} = 5 \times 10^4 \beta\emptyset\rho_f\sqrt{\frac{KT}{\rho_s d_s}}f(T, \emptyset) \tag{14}$$

The convective heat transfer coefficient is given by:

$$h = \frac{Q}{A\Delta T} \tag{15}$$

Where Q is the heat flux and ΔT is T_H-T_C

$$Nu = \frac{hL}{K_{eff}} \tag{16}$$

Where L is the characteristic length

Rayleigh number is defined as:

$$Ra = \frac{g\beta L^3 \Delta T}{\alpha \nu} \tag{17}$$

Where β is the thermal expansion, α is the thermal diffusivity and ν is the kinematic viscosity $= \frac{\mu}{\rho}$, $\alpha = \frac{K}{\rho C_p}$

The thermophysical properties of the nanoparticles are shown in Table (4.1)

Table 1 Nanoparticles thermophysical properties

Nanoparticle	Density Kg/m^3	Thermal conductivity $w.m^{-1}.k^{-1}$	Specific heat $J.kg^{-1}.k^{-1}$
Al2O3	3950	35	765
Cu	8933	400	385
TiO2	4250	8.93	686.2

Numerical procedure

The CFD code used in this investigation is ANSYS 15 as described in Chapter 3. The nanofluid is modelled as single phase model. Equations (4), (5), (6) and (14) have been used to model the density, specific heat, thermal conductivity and viscosity respectively. The laminar model was used in the natural convection simulation. For pressure velocity coupling, Courant number=200, under relaxation factor was chosen 1 for density, body force and energy. Explicit relaxation factor 0.75 for momentum and pressure, body force weighted for pressure spatial discretization, the time step=0.021 s, number of time steps=17000, the transient formulation is first order implicit, the hot and cold temperature for boundary conditions are 274 k and 273 k respectively

Grid independency study

A grid independence test was carried out in order to ensure that the solution obtained is mesh independent. The simulations were first done for various meshes with different number of cells and the average Nu was calculated for each mesh. The five meshes tested with Nu results are shown in Table 2. As it can be seen that Nu number for mesh 4 with 10700 cells found remain unchanged, and hence mesh 4 was selected for the present numerical simulations.

Table 1 Mesh dependency test results

Mesh	Number of cells	Nu
Mesh 1	6400	1.864
Mesh 2	8400	2.013
Mesh 3	10200	2.212
Mesh 4	10700	2.323
Mesh 5	11200	2.324

Validation of Results

The present CFD code results for the average Nusselt number for various Ra numbers along the hot wall are validated with results available in the literature for natural convection in an enclosure filled with nanofluids as presented in Tables 3

Table 1 Results Validations

Nu	Cu-water (ϕ=5%)		Al2O3-water (ϕ=2%)	
	Present study	Kahveci	Present study	Ho et al
$Ra=10^4$	2.431	2.461	2.323	2.372
$Ra=10^5$	5.072	5.136	4.769	4.700
$Ra=10^6$	9.946	10.04	9.389	9.314

The present code is further validated against the numerical simulation of of Khanafer et al. as shown in Fig. 2. It can be clearly seen that the present code is in excellent agreement with the work published in the literature.

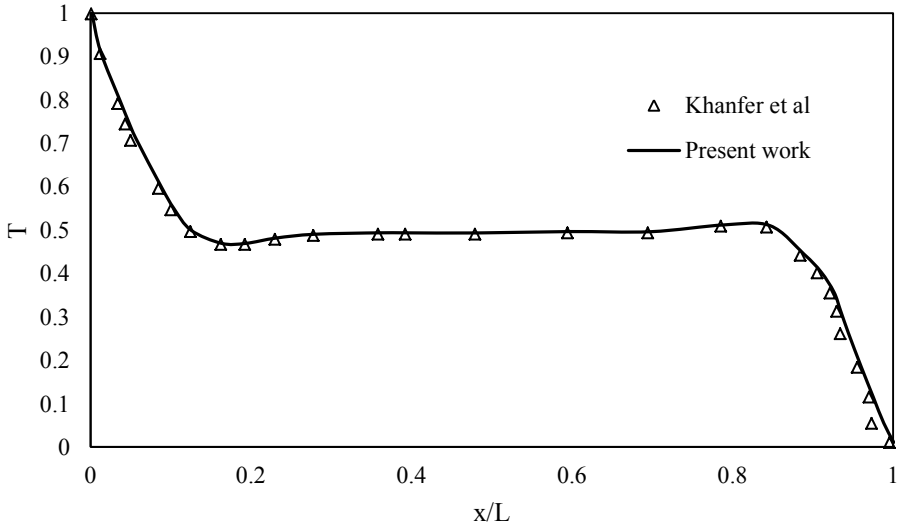

Figure 2 Results Validations

Results and Discussion

The effect of the volume fraction on the heat transfer rate is investigated for a range of Ra numbers. Four Ra number tested in the present study, Ra 1×10^4, 1×10^4, 1×10^5, 1×10^6 and 1×10^7. The volume fractions tested were between 2% and 6 %. The Nu was calculated based on two scenarios: The first scenario where Brownian motion is taken into account. The second scenario, no Brownian motion effect was considered. The results for these investigations are shown in Fig 3. The figure shows the variation of Nu number as Y axis against the volume fraction ϕ as X axis. The Nu number as shown in the figure decreases as the volume fraction decreases for all Ra numbers. This agrees well with many previously work reported in the literature. This decrease is not in favour of heat transfer convection as the increase in Nu number is an indication of the heat transfer enhancement.
This deterioration in the heat transfer is more clear in higher Ra number. This decline is less significant in Ra number 1×10^4 and 1×10^5. However, the increase in Ra number led to an increase in Nu number. As shown in the figure, Ra 1x10e^7 showed the highest Nu and subsequently the highest heat transfer rate, while Ra 1x10e^4 had the lowest Nu number.

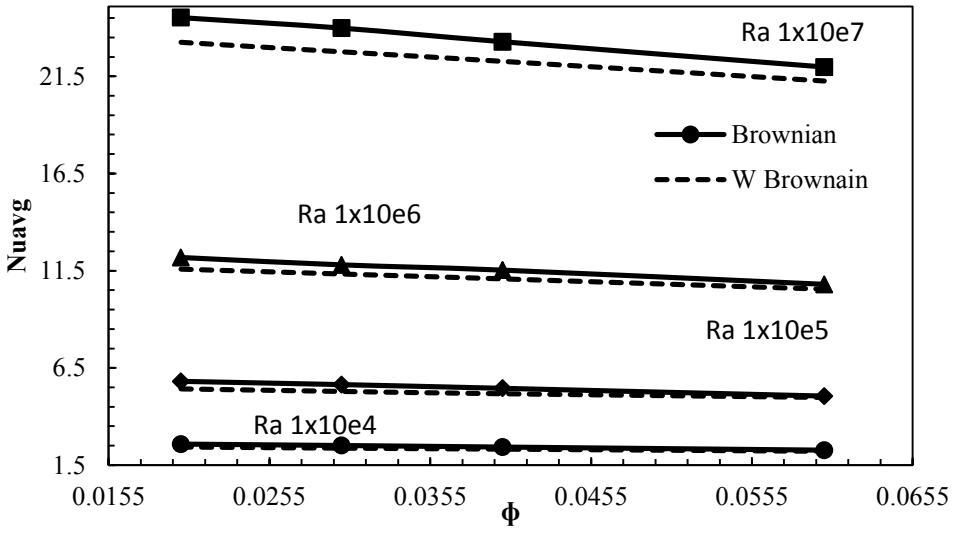

Figure 3 Change of Nu vs volume fraction

The effect of the Brownian motion was also investigated and the results are shown in the Figure. The Nu number calculated with Brownian motion is higher, this due to the increase in the thermal conductivity as a result of Brownian effect. This is attributed to the increase in thermal conductivity in equation (7), as it is well established that the increase in thermal conductivity results in an increase in Nu number. This increase is obvious in Figure 3 for Ra numbers, 1×10^6 and 1×10^7, the higher Ra numbers is accompanied with higher velocities in the near wall region, these higher velocities promote the heat transfer rate.
The figure shows that the effect of the volume fraction on Nu number is noticeable at high Rayleigh number than at low Rayleigh number. This is associated with the conduction dominated mechanism for heat transfer at low Rayleigh number compared to convection mechanism at higher Rayleigh number. Though the buoyancy force increases and exceeds the viscous forces, and hence, heat transfer is dominated by convection at high Rayleigh number
In order to have a better understanding of the effect of the nanoparticles on the heat performance, the variation of Nu number with Ra number for various nanoparticles was investigated and the results are depicted in Figure 4. The investigations were done for three nanofluids with water base fluid and three different nanoparticles Cu, TiO2 and Al2O3. The results are shown for constant volume fraction (2%) and aspect ratio .1
The Nu number was found to increase with the increase in Ra number for all nanoparticles tested,

the difference between the nanoparticles is presented in thermophysical properties which are shown in Table 4.1. All nanofluid showed similar results, however Al2O3-water nanofluid presented 2 % higher than TiO2 where Cu showed the lowest heat transfer rate with 4% compared to Al2O3-water nanofluid. It is worth to mention that all Ra numbers tested in the present study are in the laminar flow as turbulent flows are in the range > 10^8

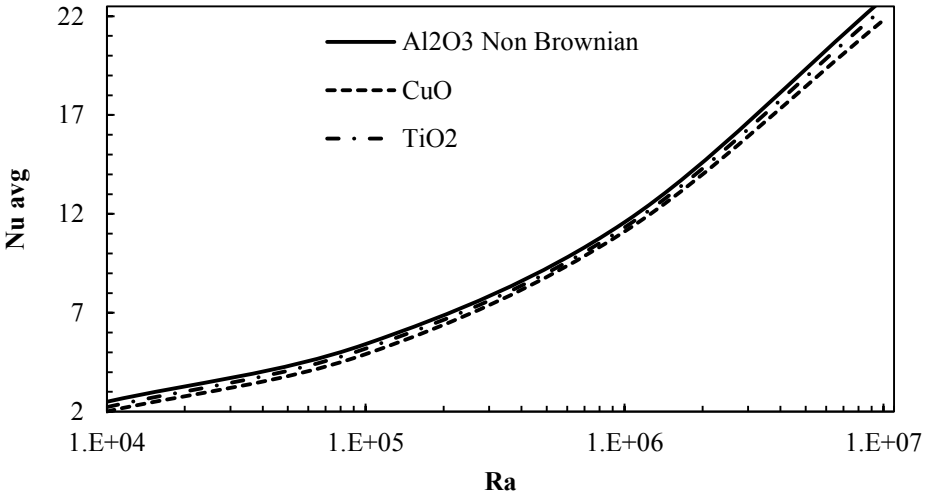

Figure 4 Effect of Nanoparticles on the heat transfer rate

The results clearly indicate that the heat transfer is less sensitive to the nanoparticle type compared to the Ra number effect. As shown in Fig 3 and 4 the increase in Ra number lead to increase in the heat transfer rate. This increase in heat transfer is due to the sensitivity of the boundary layer thickness to the higher Ra number, where for lower Ra numbers, the boundary layer thickness is insensitive to Ra number.

The effect of the Brownian motion along with the nanoparticle type on the heat transfer for a range of Ra numbers is also investigated and the results are presented in Fig 5.

The three different nanoparticles Cu, TiO2 and Al2O3 are used with water as nanofluids. The Brownian motion is considered and incorporated through the effective thermal conductivity of the nanofluids tested. The results highlight that the Nu number is enhanced with the increase in Ra number, and this increase is evident for all nanoparticles tested. However, when considering the Brownian motion the variation of Nu is almost the same for all nanofluids at low Ra numbers, where for Ra number higher than 1×10^6.

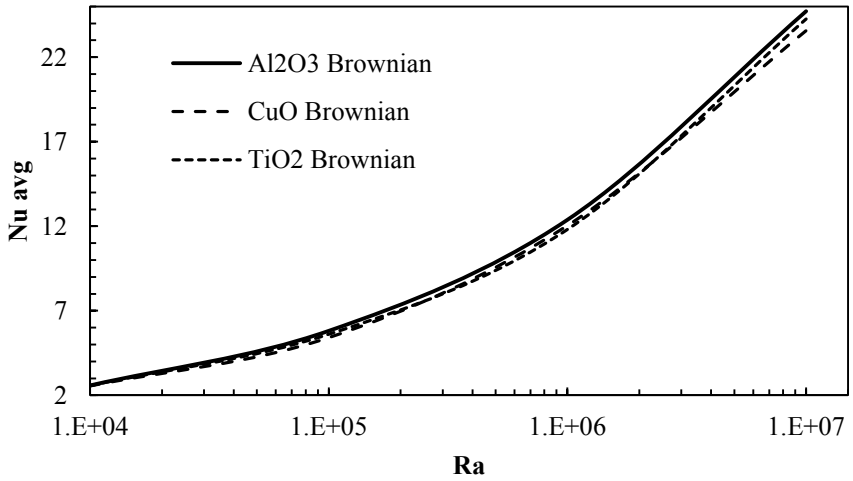

Figure 5 The effect of Brownian motion and the nanoparticle on Nu

As seen in Fig 5, at Ra number 1×10^7 the change in Nu is up to 4.6%. This increase could be attributed to the high thermal conductivity of Al2O3 nanoparticle compared to TiO2 (35 to 8.93), and also to the high specific heat of Al2O3 compared to Cu (765 TO 385). By comparing results in Fig 4 and 5, it is obvious that the Nu number is higher when considering the Brownian motion; however the heat transfer enhancement is less sensitive to the nanoparticle type when taking Brownian motion effect into account.

In natural convection, the understanding of the velocity change is essential. The flow velocity variation is investigated thoroughly for all Ra numbers. The investigations covered four volume fractions for Al2O3-water nanofluid (ϕ 2,3,4 and 6%). The results are shown in Fig 6, Fig 7, 8 and 9.

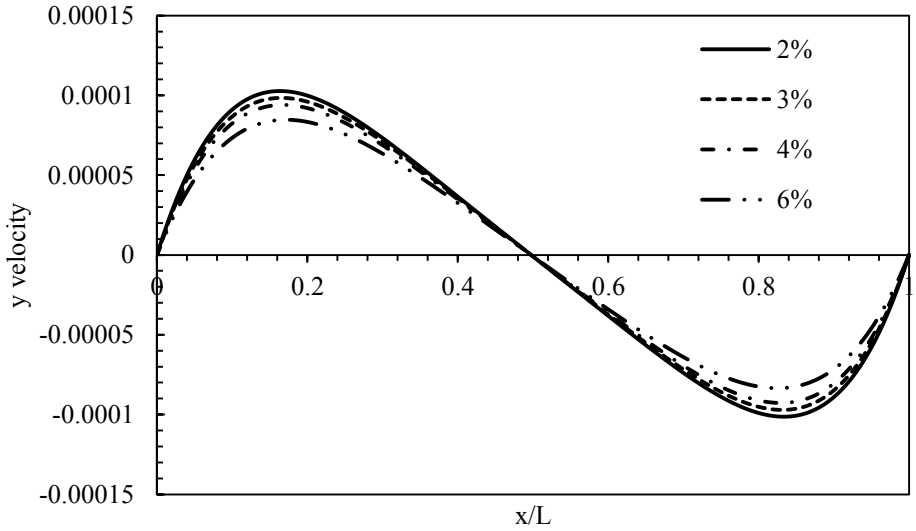

Figure 6 Velocity variation for Ra 1x104

The distribution of the vertical velocity component with the normalized distance x/L for Ra $1x10^4$ is plotted in Fig 6. The trend is consistent with the expected behavior in the natural convection phenomenon in an enclosure. The origin in the graph represents the middle of the hot wall which is located on the left of the square enclosure. The middle of the cold wall located at normalised distance equal to 1. The flow accelerates from the hot wall to the cold wall due to the buoyance forces which are the main influence of the natural convection. This buoyance force is resulted from the temperature difference between the hot and cold walls. The volume fraction 2% showed the highest velocity among the other volume fractions tested. It can be clearly seen that the increase in the volume fraction decreased the vertical velocity component. This finding is explained by the deterioration of the heat transfer due to the increase in volume fraction, as the increase in the velocity in the thermal boundary layer region is accompanied by an increase in the heat transfer rate.

This is further investigated for other Ra number. Fig 7 illustrates the variation of the vertical velocity component with the volume fractions 2,3,4,6 % for Ra $1x10^5$.

The velocity profile as depicted in the Fig 7 is found to decrease with the increase in the volume fraction. This has a negative impact of the heat transfer performance as the effective viscosity is more pronounced in natural convection as seen in equation 13 where viscosity is increased with the increase in volume fraction. Despite the increase in thermal conductivity which promotes heat transfer, the augmentation in viscosity is significant and hence the Nu number is affected by the increase in the viscosity.

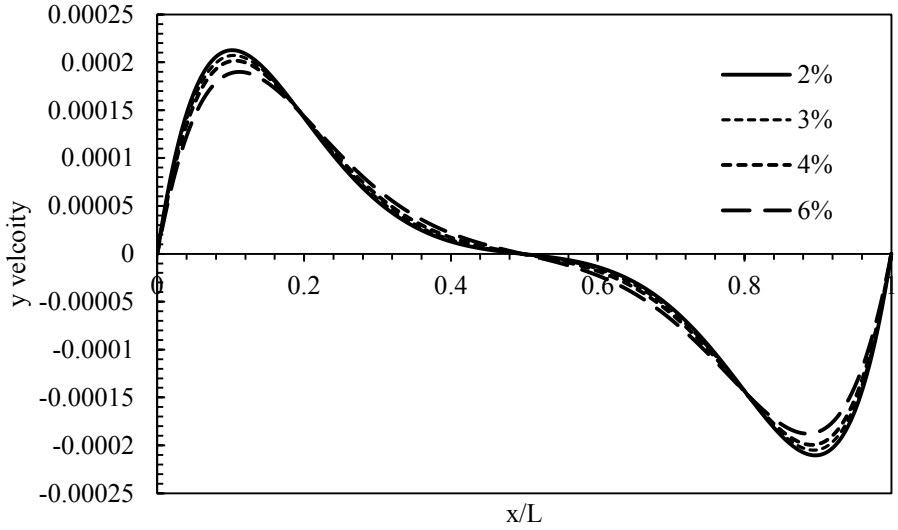

Figure 7 Velocity variations with volume fraction for Ra $1x10^5$

A similar finding is reported in Fig 8 and 9. The vertical velocity component shows a parabolic variation near the isothermal wall due to the buoyant flow inside the enclosure.
It was also found that the vertical velocity profile is insensitive to the nanoparticle type, as the three nanofluids tested showed similar vertical velocity component profile. This is attributed to the influence of the volume fraction on the effective viscosity where the nanoparticle effect has no influence on it

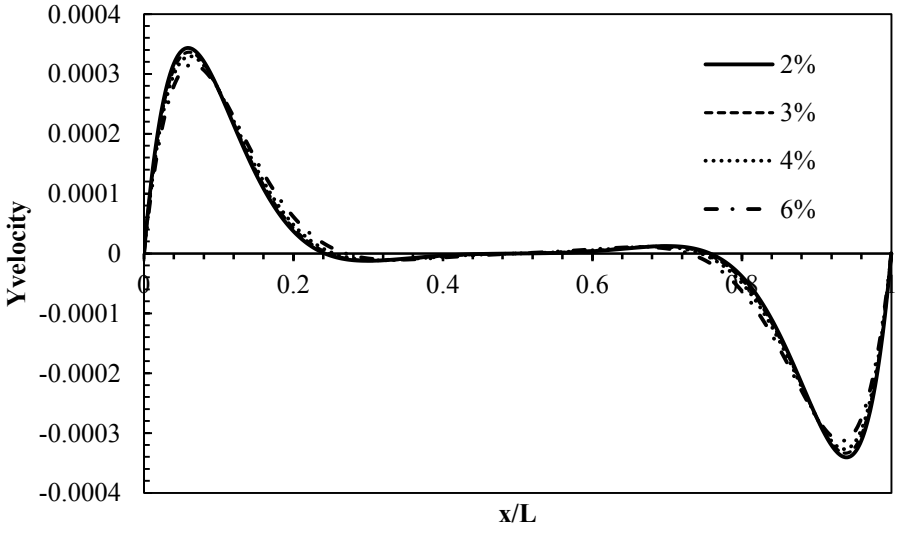

Figure 8 Variation of velocity with volume fraction for Ra $1x10^6$

Although the higher volume fraction showed less velocity on the hot wall, its corresponding velocity on the cold wall is higher. This change in flow field is directly affected by the particle suspension; however the flow velocity in the cavity canter is almost zero. This vertical velocity component profile helps in understanding of the direction of the flow rotation.

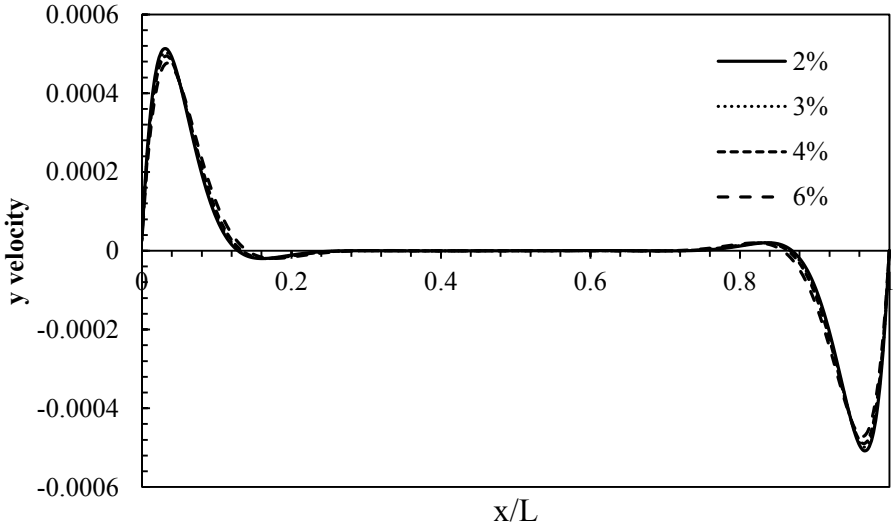

Figure 9 Velocity variation with volume fraction for Ra $1x10^7$

It should also be noted that as the Ra number increase, the velocity increase. The results in Fig 10 show clearly this velocity change. The volume fraction used in the graph shown is 2%, the Brownian effect was considered in this case. From the graph shown, it can be seen that the convection term is more pronounced at higher Ra number in the isotherm walls, i.e. in the near wall region where the velocity is almost zero in the normalized distance in the enclosure in the range 0.2-0.8

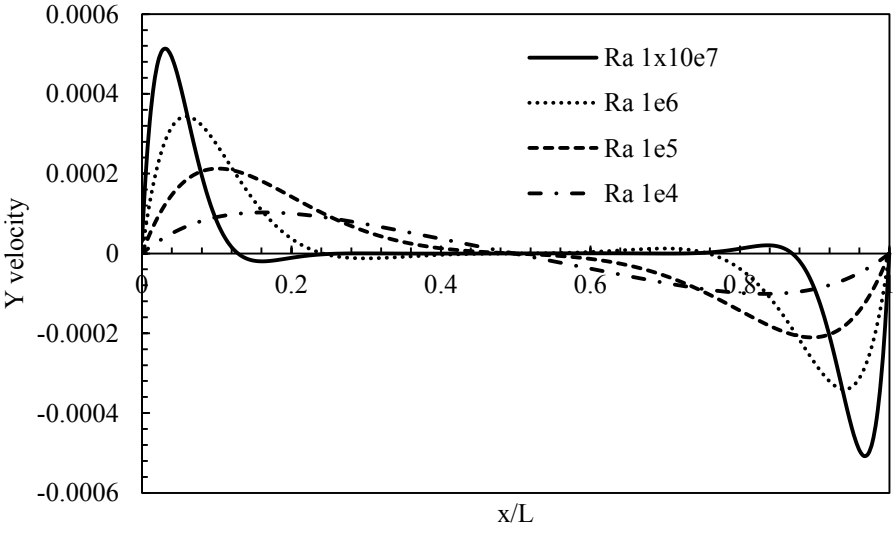

Figure 10 The velocity change with Ra number

The change the velocity for various Ra number tested in the present investigation can lead to a better understanding of the enhancement of the heat transfer due to the Ra growth, as the velocity is more pronounced in the viscous layer in the higher Ra number, so the viscosity increase effect becomes less and subsequently the heat transfer promoted. On the other hand, the volume fraction effect on the heat transfer rate was negative, so the heat transfer rate deteriorated with the increase in the volume fraction as reported by many previous works in the literature. However with no solid explanations for this influence, some researchers attributed this to the strong effect of the viscosity in the naturel convection where viscosity increases with the increase in the volume fraction as can be seen in equation 4.13 this augmentation in viscosity is accompanied with increase in thermal conductivity due to the increase in volume fraction.

The shear stress effect was also investigated in this study. In order to gain a good understanding, the velocity gradient du/dx and dv/dy are studied for different Ra numbers. The effect of the volume fraction was also investigated. The results are presented in Fig 11, 12 and 13 for Ra $1x10^4$, Ra $1x10^6$ and Ra $1x10^7$ respectively. The simulations are devoted to Al2O3-water nanofluid only as the nanoparticle type effect on the velocity was neglected as discussed earlier.

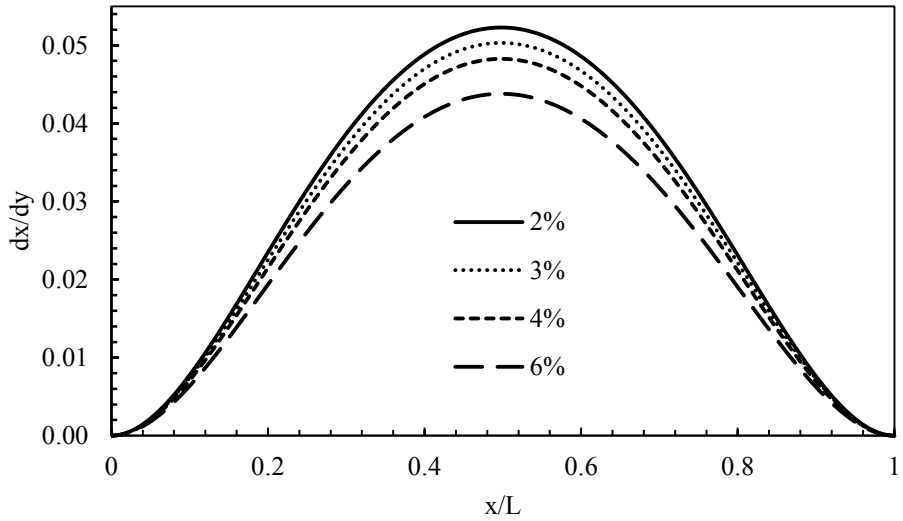

Figure 11 The variation of velocity gradient with volume fraction for Ra $1x10^4$

The axial velocity gradient is zero at the hot and cold wall and its maximum value located at the centre of the enclosure. This implies that the axial velocity is zero at the isothermal wall. As noted in the graph, the velocity gradient increases with the decrease in the volume fraction. This is explained by the increase in the viscous effect due to the particle suspension. This variation applies to all Ra number tested. However it was also noted that the increase in Ra number led to decrease in the axial velocity gradient at constant volume fraction. Another interesting finding, which represents in the variation of the axial velocity gradient at the middle of the enclosure, as the increase in Ra number, the peak of the parabola gradually, goes down as the Ra grows. At Ra $1x10^7$ two peak values were noticed for the axial velocity gradient. These two values are explained by the big change in the velocity in middle of the enclosure

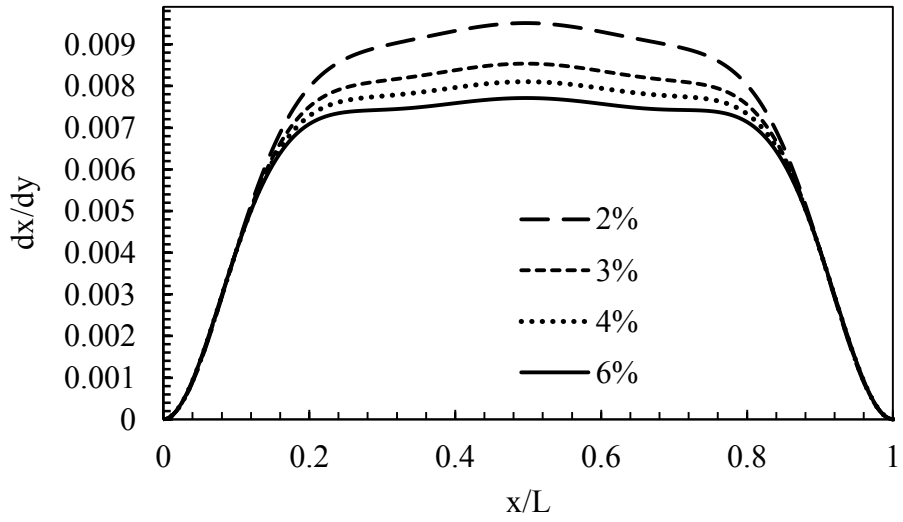

Figure 12 The variation of velocity gradient with volume fraction for Ra 1x106

It is also worthy to mention that the effect of the volume fraction is more pronounced at the centre of the enclosure where at the isothermal walls, the axial velocity gradient is insensitive to the volume fraction, this is attributed to the sharp fall of the velocity in the near wall region.

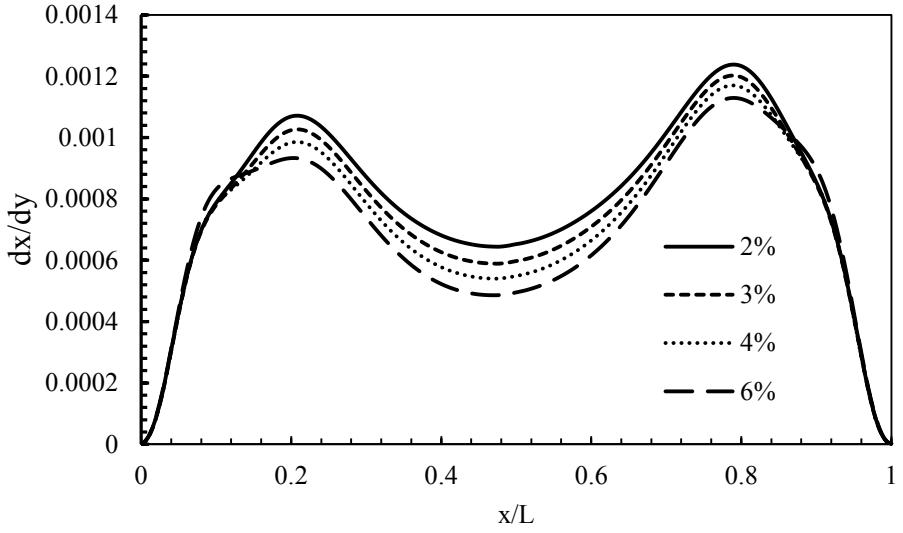

Figure 13 The variation of velocity gradient with volume fraction for Ra $1x10^7$

The Fig 14, 15, 16 and 17 illustrate the change of the velocity gradient for the vertical component at the centre line of the enclosure for a range of volume fractions for Ra $1x10^4$, $1x10^5$, $1x10^4$, $1x10^6$ and $1x10^7$ respectively. It was found that the velocity gradient increase with the increase in the volume fraction at the isotherm walls (the hot and the cold) and decreases with the increase in the volume fraction in the middle of the enclosure and this agrees well with the previous finding where the velocity has a minimum value at this location.

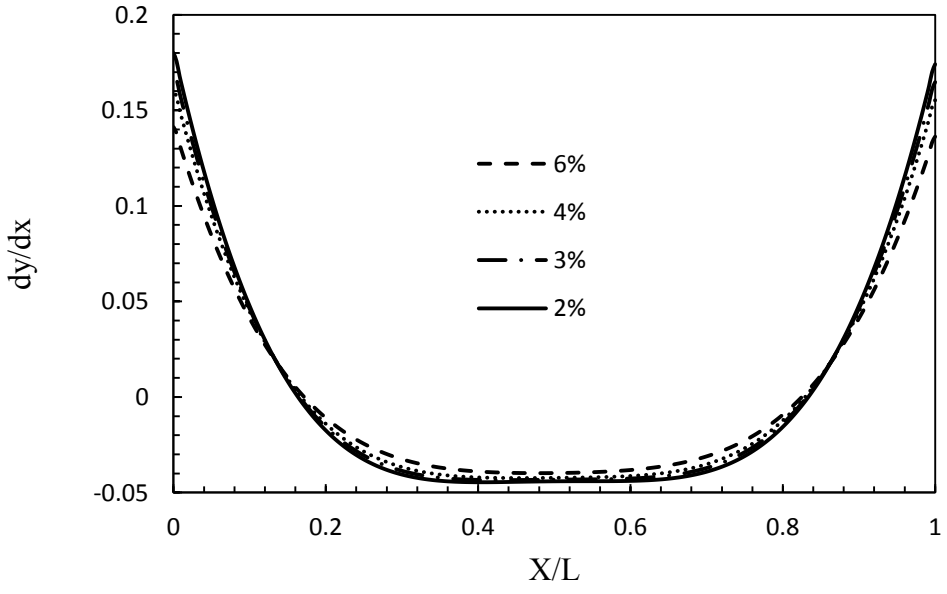

Figure 14 The velocity gradient variation with the volume fraction for Ra $1x10^4$

The vertical velocity gradient has the maximum value at the isothermal walls. The explanation for this is, when looking the shear stress equation (20) as the maximum shear stress is located at the walls. As a result at the thin fluid layer the velocity gradient and shear stress are large, where out the boundary layer both the shear stress and the velocity gradient are negligible.

$$\tau = \mu \frac{dv}{dx} \tag{18}$$

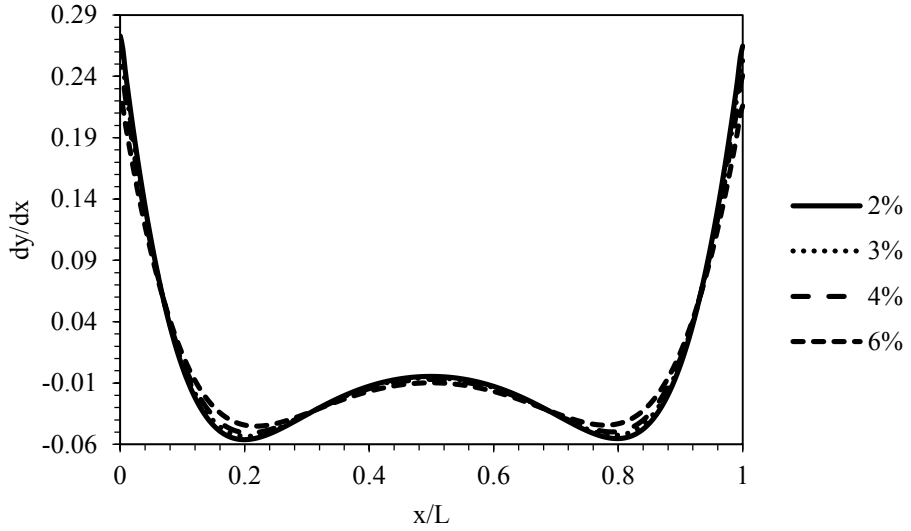

Figure 15 The variation of velocity gradient with volume fraction for Ra 1x10^5

As the Ra number rise, the vertical velocity component becomes less sensitive to the volume fraction of the particles. At which case the convection effect is more prominent where the viscous effect is declined considerably.

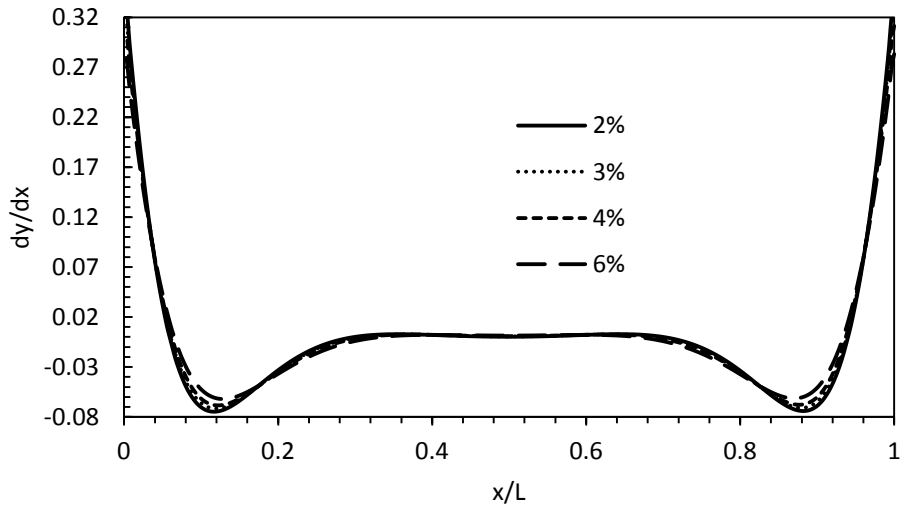

Figure 16 The variation of velocity gradient with volume fraction for Ra 1x106

In order to understand the relation between the velocity gradient and Ra, Fi 18 is introduced and it depicts the variation of different Ra numbers at the middle line of the enclosure with velocity gradient at a constant volume fraction (ϕ=2%). It is clearly seen that as Ra increases the velocity gradient increases in the near wall region where shear stress has the maximum value. However when the boundary layer increases, the velocity gradient decreases with the increase in the Ra number particularly in the normalised distance ranges (0.056-0.196) and (0.844-0.984). This opposite effect is attributed to decline in the viscous effect with the grow in the boundary layer thickness.

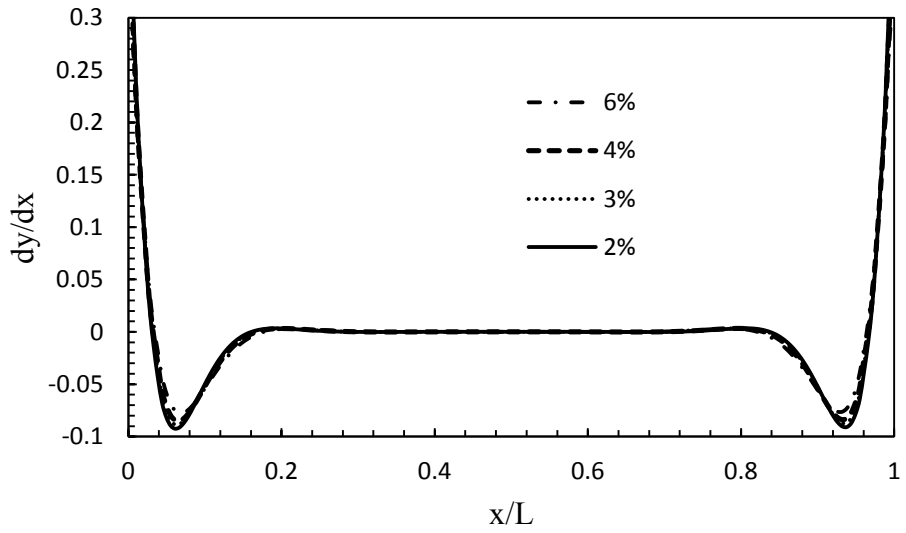

Figure 17 The variation of velocity gradient with volume fraction for Ra 1x107

With increasing distance from the isothermal walls, the viscosity effect vanishes gradually to the location where the velocity gradient promotes again with the Ra enhancement. This augmentation is explained by the dominant of the buoyant forces over the viscous forces in the circulation inside the enclosure.

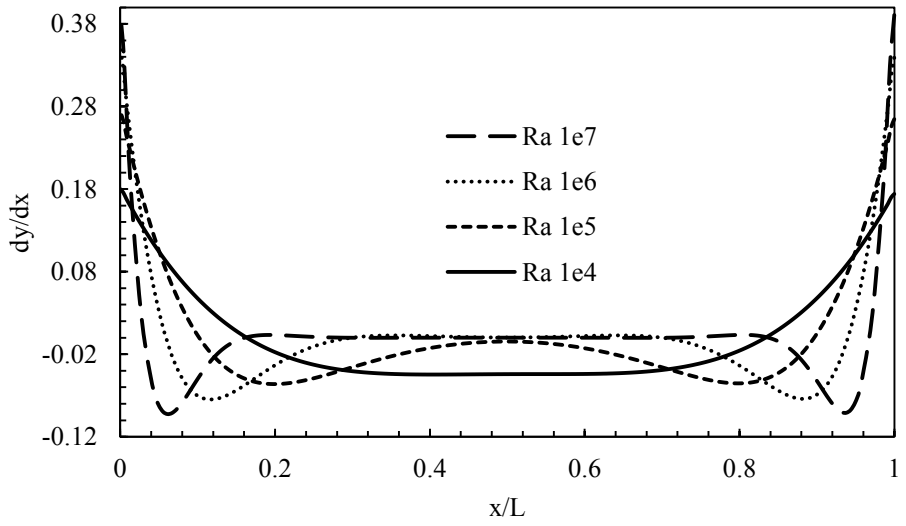

Figure 18 Ra number change with velocity gradient

In order to give a better understanding of the flow circulation and how the heat performance affected, the contours of the temperature is presented for Ra 1x104, 1x105, 1x106 and 1x107 in Fig 19 a, b, c and respectively. It is well established that due to the buoyancy effect and the gravitational force the flow moves in the enclosure from the hot wall to the cold wall

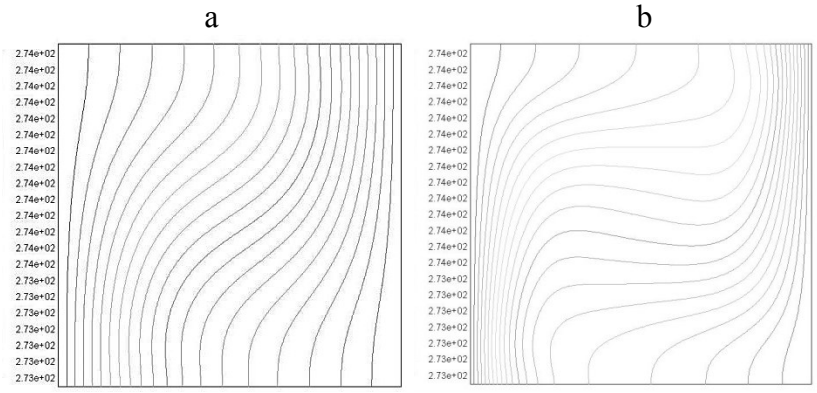

This motion can be visibly seen in the different Ra contours. However it was noted that with the increase in Ra number, the flow advances steeply which aproved by the increase in the vertical velocity component as discussed earlier. This rise is accompained with a heat transfer enhancement.

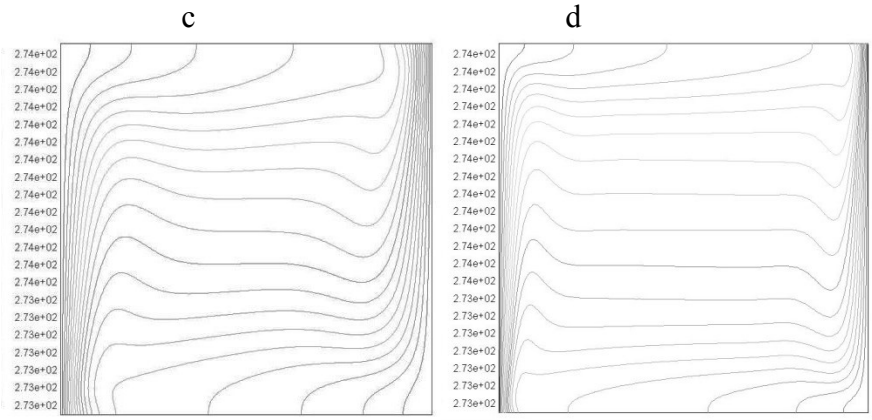

Figure 19 Isotherm contours for a) Ra1x104. b) Ra 1x105. c) Ra 1x106. d) Ra 1x107

Conclusion

The natural convection problem with Brownian motion utilizing various nanofluids was investigated and the results were presented and discussed.
Four Ra numbers were tested in the present study, Ra $1x10^4$, $1x10^5$, $1x10^6$ and $1x10^7$, and a range of volume fractions from 2% to 6%.
The heat transfer was deteriorated with the increase in the volume fraction of the nanoparticle and this applies to all nanoparticles.
The heat transfer improved by the increase in the Ra number. The effect of the Brownian motion was also investigated and the results showed that the Brownian motion effects are pronounced in the higher Ra numbers, however the heat transfer with Brownian motion showed an improvement compared to that when the Brownian motion is neglected.
The velocity gradients were studied and the results showed that the velocity gradient was influenced by the volume fraction of the nanoparticles.
The various nanoparticles tested in the present study showed similar behaviour of heat transfer performance. However, this effect is clearly seen compared to the case where no Brownian motion effect is considered, particularly at higher Ra numbers.

Nomenclature

A	Area [M2]
K	Thermal Conductivity [W/M2K]
Q"	Heat Flux [W/M2K]
CP	Specific Heat at Constant Pressure [KJ KG-1 K-1]
C_F	Skin Friction Factor
D	Diameter m
μ	Viscosity [KG m^{-1} s^{-1}]
ρ	Density [KG.m^{-3}]
ϕ	Volume Fraction
T	Temperature [^{O}K]
h	Heat Transfer Coefficient
L	Length [m]
Re	Reynolds Number=UDρ/μ
Nu	Nusselt Number=hD/K

References

AMINOSSADATI, S. M. & GHASEMI, B. 2009. Natural convection cooling of a localised heat source at the bottom of a nanofluid-filled enclosure. *European Journal of Mechanics - B/Fluids,* 28**,** 630-640.

CHOI, S. U. S. & EASTMAN, J. A. 1995. *Enhancing thermal conductivity of fluids with nanoparticles*.

CORCIONE, M., HABIB, E. & QUINTINO, A. 2013. A two-phase numerical study of buoyancy-driven convection of alumina–water nanofluids in differentially-heated horizontal annuli. *International Journal of Heat and Mass Transfer,* 65**,** 327-338.

ETAIG, S., HASAN, R. & PERERA, N. 2016. Investigation of a New Effective Viscosity Model for Nanofluids. *Procedia Engineering,* 157**,** 404-413.

GHASEMI, B. & AMINOSSADATI, S. M. 2009. Natural Convection Heat Transfer in an Inclined Enclosure Filled with a Water-Cuo Nanofluid. *Numerical Heat Transfer, Part A: Applications,* 55**,** 807-823.

GHASEMI, B. & AMINOSSADATI, S. M. 2010. Brownian motion of nanoparticles in a triangular enclosure with natural convection. *International Journal of Thermal Sciences,* 49**,** 931-940.

HO, C. J., LIU, W. K., CHANG, Y. S. & LIN, C. C. 2010. Natural convection heat transfer of alumina-water nanofluid in vertical square enclosures: An experimental study. *International Journal of Thermal Sciences,* 49**,** 1345-1353.

KHANAFER, K., VAFAI, K. & LIGHTSTONE, M. 2003. Buoyancy-driven heat transfer enhancement in a two-dimensional enclosure utilizing nanofluids. *Int J Heat Mass Transf,* 46**,** 3639 - 3653.

KOO, J. & KLEINSTREUER, C. 2004. A new thermal conductivity model for nanofluids. *Journal of Nanoparticle Research,* 6**,** 577-588.

MANCA, O., MUSTO, M. & NASO, V. Natural convection on a vertical isoflux plate with a downstream unheated extension and a parallel shroud. ASME-IMECE, 2001. 103-112.

NASRIN, R., ALIM, M. A. & CHAMKHA, A. J. 2012. Buoyancy-driven heat transfer of water–Al2O3 nanofluid in a closed chamber: Effects of solid volume fraction, Prandtl number and aspect ratio. *International Journal of Heat and Mass Transfer,* 55**,** 7355-7365.

OZTOP, H. F. & ABU-NADA, E. 2008. Numerical study of natural convection in partially heated rectangular enclosures filled with nanofluids. *International Journal of Heat and Fluid Flow,* 29**,** 1326-1336.

PUTRA, N., ROETZEL, W. & DAS, S. 2003. Natural convection of nano-fluids. *Heat and Mass Transfer,* 39**,** 775-784.

SALEH, H., ROSLAN, R. & HASHIM, I. 2011. Natural convection heat transfer in a nanofluid-filled trapezoidal enclosure. *International Journal of Heat and Mass Transfer,* 54**,** 194-201.

SARRIS, I. E., LEKAKIS, I. & VLACHOS, N. S. 2004. Natural convection in rectangular tanks heated locally from below. *International Journal of Heat and Mass Transfer,* 47**,** 3549-3563.

SUN, Q. & POP, I. 2011. Free convection in a triangle cavity filled with a porous medium saturated with nanofluids with flush mounted heater on the wall. *International Journal of Thermal Sciences,* 50**,** 2141-2153.

XUAN, Y. & LI, Q. 2000. Heat transfer enhancement of nanofluids. *Int J Heat Fluid Flow,* 21**,** 58 - 64.